01,07

Nonlinear dynamics of an individual Portevin–Le Chatelier deformation bands

© A.A. Shibkov, A.E. Zolotov, M.F. Gasanov, A.A. Denisov, R.Y. Koltsov, S.S. Kochegarov

Tambov State University,
Tambov, Russia

E-mail: shibkovaleks@mail.ru

Received July 8, 2022
Revised July 8, 2022
Accepted July 9, 2022

Based on high-speed studies of the dynamics of Portevin–Le Chatelier ambryo bands with a temporal resolution of up to 20 μs and a spatial resolution of up to 10 μm/px, their classification is proposed, which includes four types of bands depending on the nature of interaction with other bands and the sample surface (using the example of a polycrystalline aluminum-magnesium alloy). It has been found that all types of ambryo bands demonstrate nonlinear dynamics with a sharp acceleration of the band tip and the growth rate of its volume at the final stage before reaching the sample surface. A phenomenological model of the nonlinear growth of the ambryo band is proposed, which explains the exponential self-acceleration stage observed experimentally. The sharp absorption of acoustic noise at the stage of accelerated band growth is discussed.

Keywords: nonlinear dynamics, Portevin–Le Chatelier effect, deformation ambryo bands, acoustic emission, dislocation mobility, aluminum-magnesium alloy.

DOI: 10.21883/PSS.2022.11.54178.429

1. Introduction

Discontinuous deformation of metals and alloys — the Portevin–Le Chatelier (PLC) effect — is a vivid non-linear phenomenon in the physical material science that consists in spontaneous (self-organizing) autolocalization of plastic deformation in dynamically determined situations with defined deformation rate $\dot{\varepsilon}_0$ or stress rate $\dot{\sigma}_0$, respectively [1–7]. The interest in discontinuous deformation and band generation is related not only to the study of non-linear effects in the macrokinetics of plastic materials due to spatial-time self-organizing of large dislocation ensembles, but also to the practical application of metal alloys demonstrating the PLC effect (alloys based on aluminum, copper, titanium, zirconium, medium-alloyed steel, etc., in particular, high-technology aluminum alloys used in aerospace and transport industries). Macroscopically localized deformation bands compromise surface quality of industrial products, cause local corrosion and directly participate in the mechanism of the main crack initiation and development [8–10].

Usually, a distinction is made between three main types of PLC bands (types A, B, C), each corresponding to a certain shape and sequence of stress serration on deformation curves [4]. Type C bands occur in randomly located positions on the sample surface and do not propagate. They are accompanied with rare stress drops of a large amplitude. Type B bands propagate in a jerk-like manner with approximately equal intervals. Type A bands propagate continuously like a solitary wave (soliton behavior) with arbitrary localized stress serrations on the tensile curve. Transitions between different band types $C \to B \to A$ and corresponding types of stress serrations take place with the growth of the deformation rate (in a range of $\sim 10^{-6}-10^{-2}\,s^{-1}$ for Al–Mg alloys at a room temperature [11–15]).

The phenomenological classification of PLC bands by propagation character proposed in [4] is based on the experimental technique of band recording with a quite narrow time and spatial resolution, i.e., TV-camera video recording with a rate of 25 fps (frames per second) and a resolution of 100 μm/px. Video recording with a rate of 500 fps and a resolution of 8 μm/px has shown that type B „jerking“ band is a time-spatial structure composed of several deformation bands, each, except the primary (mother) band, nucleating at the boundary of the preceding band and expanding in such a way that its „center of gravity“ remains immobile. As a result of the deformation hand-off from one band to another, when a new band is nucleated at the boundary of the preceding band, the macro-localized deformation propagates along the direction of sample expansion [6,16].

Further increase in the rate of video recording of the deformed sample up to 5000 fps made it possible to identify a stage of growth of the embryo band in the direction of maximum tangential stresses that make an angle of $58-63^\circ$ to the expansion axis [17–19], while video recording with a rate of 25 000 fps shows the elliptical shape of the embryo band outline and speed jerks of its tip and the moment of reaching the opposite side surface of the sample, i.e., the moment when a complete deformation band is formed [20,21]. Typical times in the evolution of the embryo band $\sim 0.1-1$ ms are less than the build-up time of the subsequent stress drop ($\sim 1-3$ ms), and hence, they are

considerably shorter than the time interval between the drops. Therefore, the processes responsible for embryo band initiation and growth are a separate target of research, which is not directly related to the dynamic behavior of types A, B, C, that are characterized by a different degree of stress recovery after yet another stress drop depending on temperature-speed conditions of the deformation.

As can be seen, an increase in time resolution by 3 orders of magnitude (from 25 to 25000 fps) and a several times increase in spatial resolution (from ~ 100 to $8\,\mu$m/px) made it possible to identify essential features of geometry and dynamics of individual deformation bands at the earliest stage of their evolution, with a duration of up to ~ 1 ms, which are independent of A, B, C type of dynamic behavior and type of test machine (stiff or soft), and therefore these features are of general character related to the nature of initiation of plastic instability resulting in the phenomenon of PLC discontinuous deformation.

Thus, in the last decade, works have been published where the first millisecond of deformation band evolution is considered as a separate target of research. Experimental study of *in situ* „millisecond dynamics" of individual band formation requires the use of methods with sufficiently high time and spatial resolution, i.e., video recording of a deformed sample surface at a rate of at least ~ 5000 fps with appropriate computer software to process the images synchronously with other quick-acting methods, for example, acoustic emission (AE) method, etc. This study is devoted to the experimental research *in situ* of embryo band evolution by video recording of the deformed sample surface at a rate of up to 50000 fps and by AE method. AlMg6 polycrystalline aluminum-magnesium alloy demonstrating explicit discontinuous deformation and band generation at a room temperature was chosen as a material for the research.

2. Procedure

Samples of industrial aluminum-magnesium alloy (AA5059) AlMg6 (Al — 6.15% Mg — 0.65% Mn — 0.25% Si — 0.21% Fe (wt.%)) shaped as double-side blades with working area dimensions of $6 \times 3 \times 0.5$ mm were machine-cut from a cold-rolled sheet along the rolling direction with subsequent annealing at a temperature of 450°C for 1 hour and water quenching. Average grain size after heat treatment was $10-12\,\mu$m. Samples were expanded in „stiff" and „soft" modes. The first mode was implemented in the Instron (3344) test machine at a speed in the range of $3 \cdot 10^{-6}-3 \cdot 10^{-3}\,\mathrm{s}^{-1}$, the second mode was implemented in serrated creep conditions at stresses of 200−330 MPa, considerably exceeding the offset yield strength of AlMg6 alloy, $\sigma_{0.2} \approx 160$ MPa.

Video recording of the deformed sample was performed by the FASTCAM Mini UX50/100 (Photron) high-speed digital video camera synchronously with changes in the deformation and force. Video recording rate was varied in a range of $(2.5-5.0) \cdot 10^4$ fps to monitor earlier stages of deformation bands generation. The sample surface was illuminated at an angle of about 30−40° by a source of white light. The optical method used is similar to the shadow method of [4] modified in two aspects: more than three orders of magnitude increase in the speed of video recording and the use of computer processing of digital images by program subtraction of successive images. This method of image processing [22] allows highlighting the contours of items (bands or cracks) moving with speeds greater than the threshold speed. Acoustic emission signals were measured using the Zetlab BC-601 AE sensor with almost flat amplitude frequency response in the frequency range of $\sim 100-800$ kHz and smooth decrease in the lower frequency range, < 100 kHz. AE signals were amplified by 40 dB using the AEP5 (Vallen-Systeme) pre-amplifier and recorded continuously without threshold with an amplitude resolution of 16 bits and a recording rate of 5 MHz.

3. Experimental results

3.1. Types of embryo bands

The analysis of video recording data for the initial generation process of more than hundred of individual deformation bands with a duration of about one millisecond in conditions of discontinuous deformation and PLC effect made it possible to classify embryo bands into at least four main types by their morphology and dynamics. The first type includes primary (mother) bands nucleating and growing in a material where there are no other deformation bands (Fig. 1, *a*). The second type includes secondary bands nucleating at the boundary of the preceding band (including the primary band), i.e., macroscopically „heterogeneously "initiating and growing along this boundary (Fig. 1, *b*). The associated embryo band growing in the direction at an angle of about 60° to preceding static bands falls into the third type of embryo bands (Fig. 1, *c*). Finally, the fourth type includes arc-shaped bands growing in the area of blades (Fig. 1, *d*).

As known, the deformation band is a mechanical charge, i.e., it contains an excess of dislocations of one mechanical sign [5]. To compensate for the corresponding bending moment, bands occur in the material with an excess of an opposite mechanical charge. These include associated bands. The associated embryo bands classified as type three bands inevitably arise in the process of sample deformation. They are characterized by unstable kinetics of growth with variations of tip speed in the areas of crossing with static bands creating a macroscopically inhomogeneous structure of dislocation pinning forces in the material where the embryo band propagates. It is worth noting, that the interaction of associated bands is important when the contraction is formed and the sample is fractured [8,9]. It can be assumed that in the case of crossing of associated bands multiple cracks occur by the Cottrell mechanism [23], which merge into a main crack under large stresses.

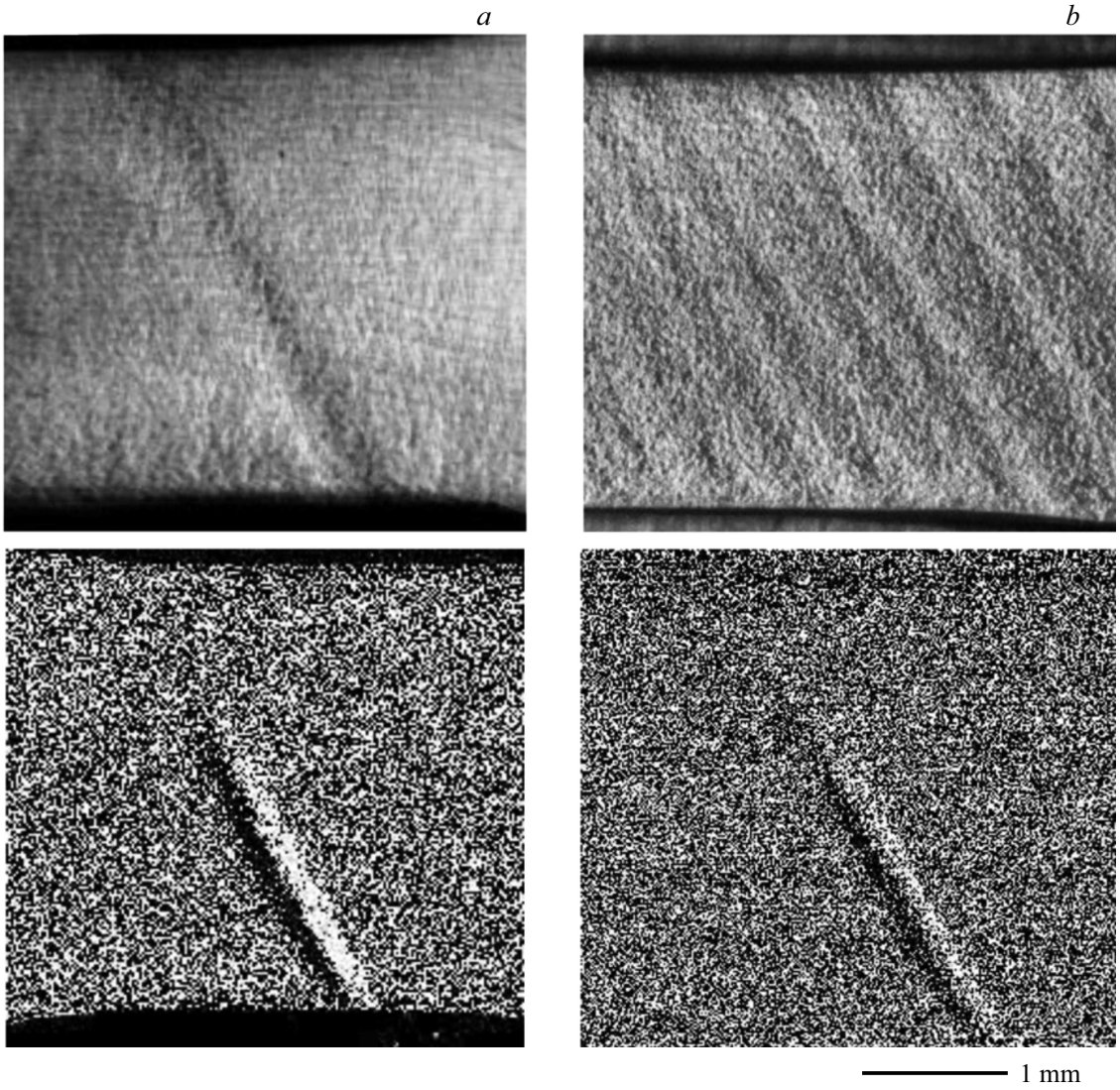

Figure 1. Types of embryo bands of deformation: *a* — primary band; *b* — band growing along the preceding static band; *c* — associated band growing across at an angle of about 60° to static bands; *d* — arc-shaped band growing in the area of blades. Top images show initial state, lower images show results of computer processing of growing embryo band images.

Arc-shaped embryo bands fall into the fourth type of bands. They grow in the area of blades where stressed state is considerably different from that in the working area of the sample, while the level of stresses is lowered due to an increased cross-section. They have the lowest speed of tip growth among the above listed types of embryo bands, which is not greater than several meters per second, while the duration of growth is the biggest, up to several milliseconds, respectively.

For comparison with the date from literature, it is worth noting, that the embryo bands as the earliest stages of PLC bands generation were observed in Al–Mg system alloys using video recording with a rate of more than 500 fps [17–21,24–27]. In early study [4], on the basis of 25 fps video recording of bands, three hypothetical scenarios for the transversal growth of an embryo band in a flat sample were proposed: a) band nucleates at a lateral sample surface with its width unchanged while growing until outlet to the opposite lateral surface; b) band with a thickness of a few atomic planes „shoots through“ the cross-section, and then expands in the direction of the expanding stresses; c) wedge-shaped embryo band crosses the cross-section in the direction of maximum tangential stresses. A scenario without band nucleation was proposed recently in [25]. The experimental data gained up to now for the dynamics of bands are rather in support of the third scenario: the embryo band in a flat sample has a shape close to a semi-ellipse, and its growth is characterized by a tip speed of υ_t and a transversal growth speed of υ_s (see [21]).

3.2. Non-linear dynamics of embryo bands

As it was determined, all types of embryo bands demonstrate non-linear dynamics with a final stage of accelerated

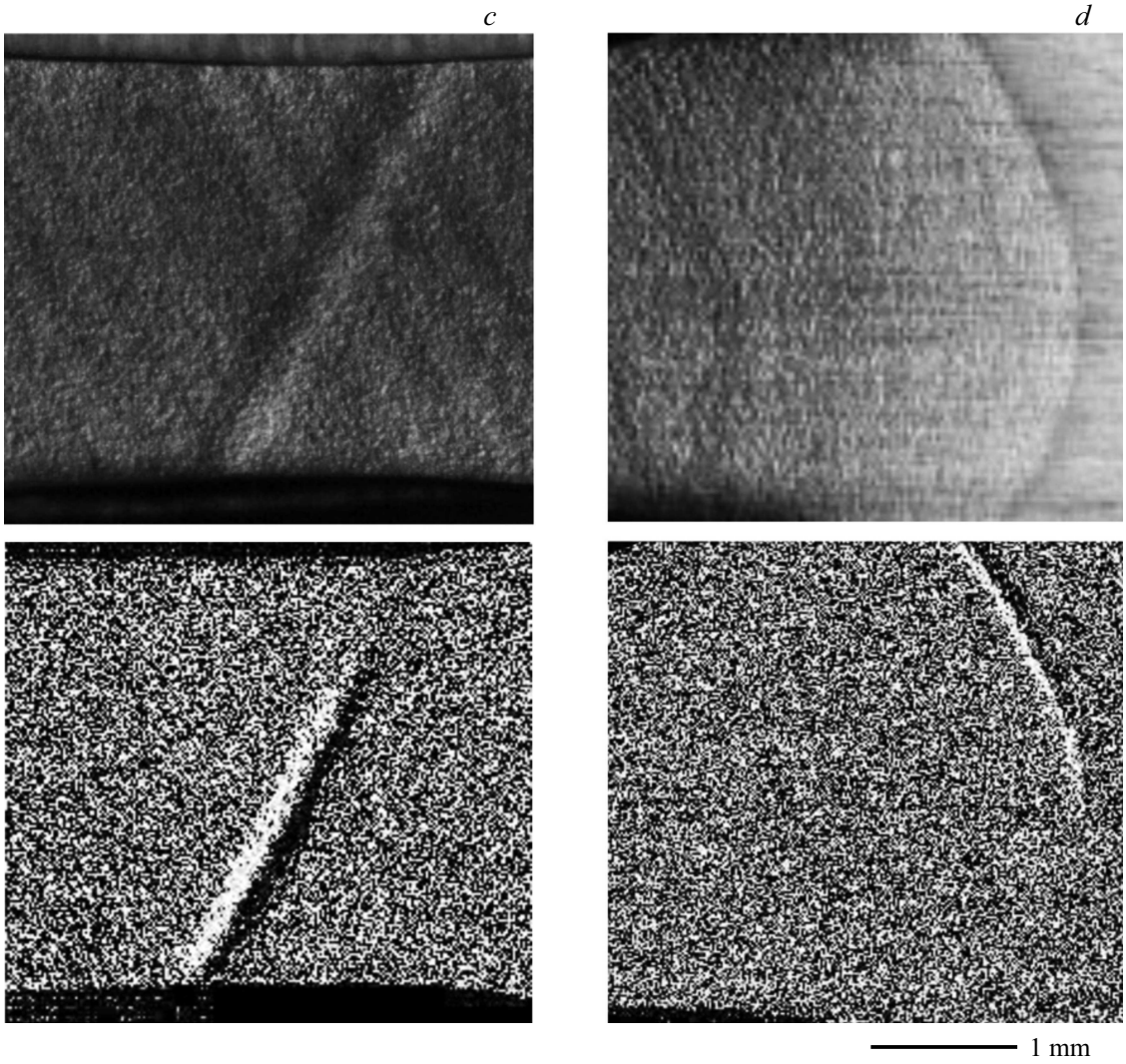

Fig. 1 (*cont.*).

growth of the band tip with the maximum tip speed taking place at the moment of reaching the opposite lateral surface of the flat sample. It is important for non-linear band behavior simulation to consider the nucleation and growth of the primary band (band of the first type) as an example of spontaneous generation of an individual band when there are no other bands at a constant level of applied stress.

Fig. 2 shows records of force response $\Delta\sigma$ (curve *1*), time dependencies of band area S_b (i.e,. the area inside the band contour), its derivative with respect to time $\dot{S}_b$ (curves *2* and *3*, respectively) and band tip speed υ_t (curve *4*), and top images are video recording frames of embryo band growth recorded at a rate of 25000 fps. The band is nucleated at the lateral surface of a flat sample (at $t = 0$). As can be seen, the needle-shaped incomplete band crosses the flat sample cross-section at an angle of about 60° to the expansion axis during the time of t_{cr} (~ 4 ms) from the moment of band nucleation. At the moment of t_{cr} the incomplete (embryo) band reaches the opposite lateral surface of the sample and becomes a „complete“ band, which then expands with a decreasing speed during several milliseconds. Angle φ between the band and the expansion axis is close to the direction of maximum tangential stresses (for isotropic plastic material the angle of φ corresponds to the condition of $\mathrm{tg}(\varphi) = \sqrt{2}$, i.e., $\varphi = 54°44'$ [28]).

At the moment of t_{cr} of the embryo band reaching the opposite surface, the band tip speed υ_t and the band area growth speed $\dot{S}_{cr}$ reach their maximum values, and the stress drop starts at $t \geq t_{cr}$. It means that the accelerated and jerk-like growth of the embryo band takes place in conditions of approximately constant applied stress, which is indicative of non-linear dynamics of the primary band in addition to the spontaneity of the band nucleation process. The subsequent relaxation of stress suppresses the speed of complete band expansion (Fig. 2, curves *1–3*).

According to video records, the embryo band tip speed first grows almost linearly $\upsilon_t \propto t^n$, where $n \approx 1.0–1.2$, and accelerates abruptly at the final stage (about ~ 1 ms). At the

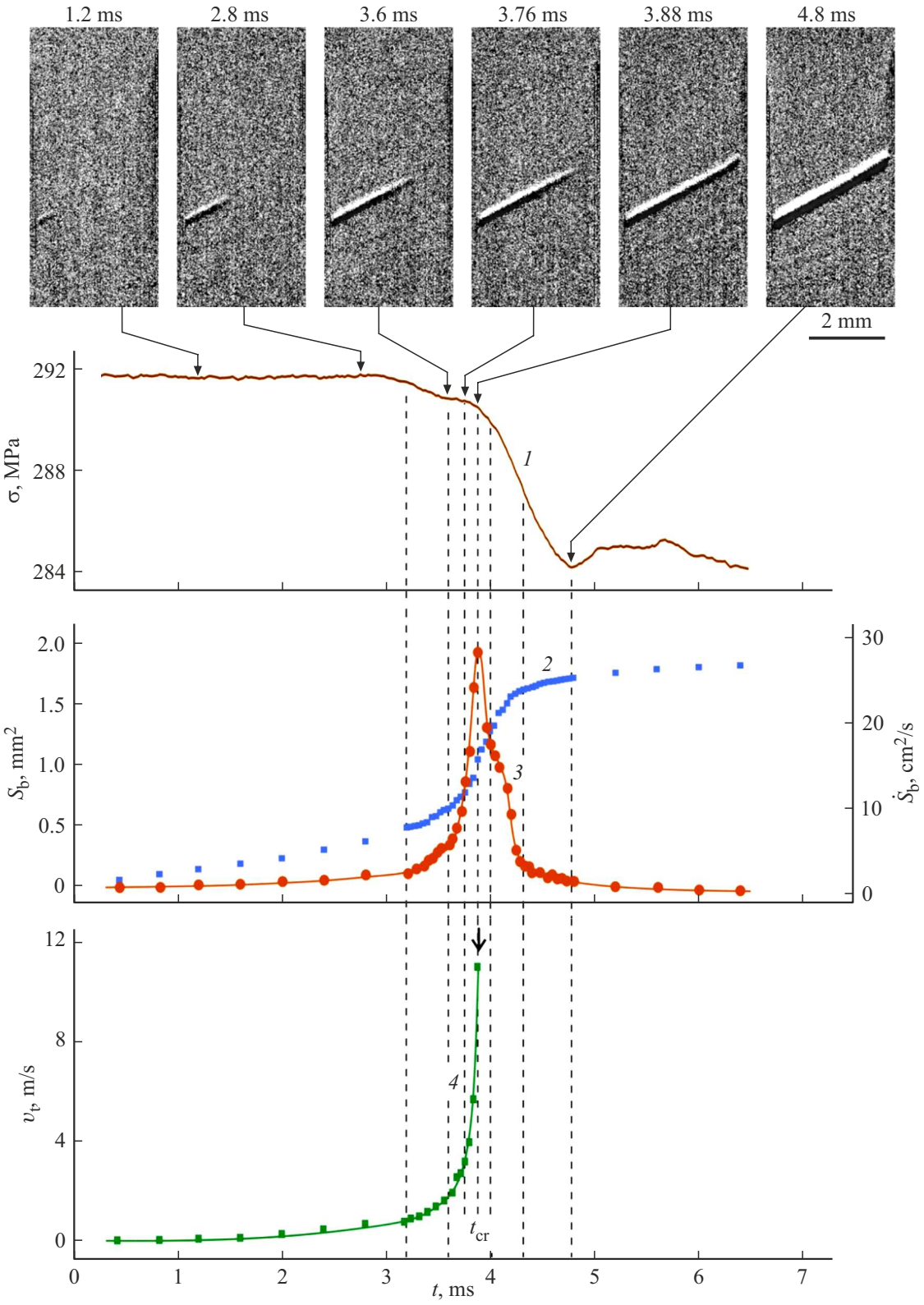

Figure 2. Dynamics of the primary embryo band (band of the first type): curve *1* — force response $\sigma(t)$; *2* — band area $S_b(t)$; *3* — band area growth rate $\dot{S}_b(t)$; *4* — band tip speed $\upsilon_t(t)$. Top — fragment of video recording of band growth through the sample cross-section. Video recording rate is 25000 fps. Arrows show the sequence of chosen video recording frames.

moment of t_{cr}, when the embryo band crosses the sample bulk, the tip speed can be as high as 10 m/s or more, while transversal speed is not greater than 10 cm/s. In the example shown in Fig. 2: $\upsilon_t(t_{cr}) \approx 12$ m/s, $\upsilon_s(t_{cr}) \approx 6$ cm/s. At the final accelerated stage of growth the time dependence of band tip speed is approximated by an exponential function

$$\upsilon_t(t) \propto \exp(t/\tau) \qquad (1)$$

with a correlation factor of 0.9981 at a time constant of $\tau = 0.13$ ms, which is indicative of positive feedback presence in the process of growth. The latter can be attributable to the growth of stress concentration near the band tip as it approaches the opposite edge of the sample. The growth of stress increases the speed of dislocation in the band head. The corresponding increase in band length decreases the „live" cross-section, which causes the further increase in stress concentration in addition to growing stresses of nonconformity between plastic deformable and non-deformable areas of material, that depend not only on the Laplacian deformation field [29], but also on the plastic flow speed gradient at the band tip. Taking into account the threshold character of the dislocation dynamics (critical stress of dislocations separation from stops, critical stresses of dislocations multiplication, etc.), the continuous growth of stress concentration at the band tip will engage new dislocations in the process of growth, which is an additional factor of the positive feedback.

Despite the more complicated character of the dynamics of other embryo band types, it also includes the final stage of accelerated growth before the band reaching the opposite lateral surface (Fig. 3). To study this stage we increased video recording rate up to 50000 fps in a special series of experiments. Synchronously with the video recording we measured the AE signal with the filtration of low frequencies at a level of 100 kHz and a recording rate of 5 MHz.

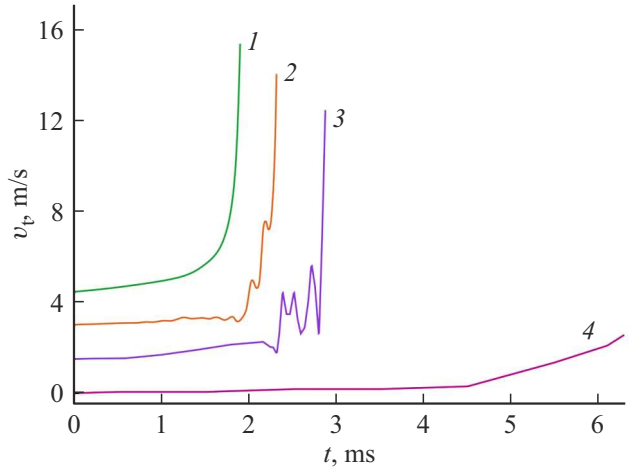

Figure 3. Final fragments of kinetic curves $\upsilon_t(t)$ of embryo band growth of the first (curve *1*), the second (*2*), the third (*3*), and the fourth (*4*) types. Curves have a 1.5 m/s offset along the axis of ordinates.

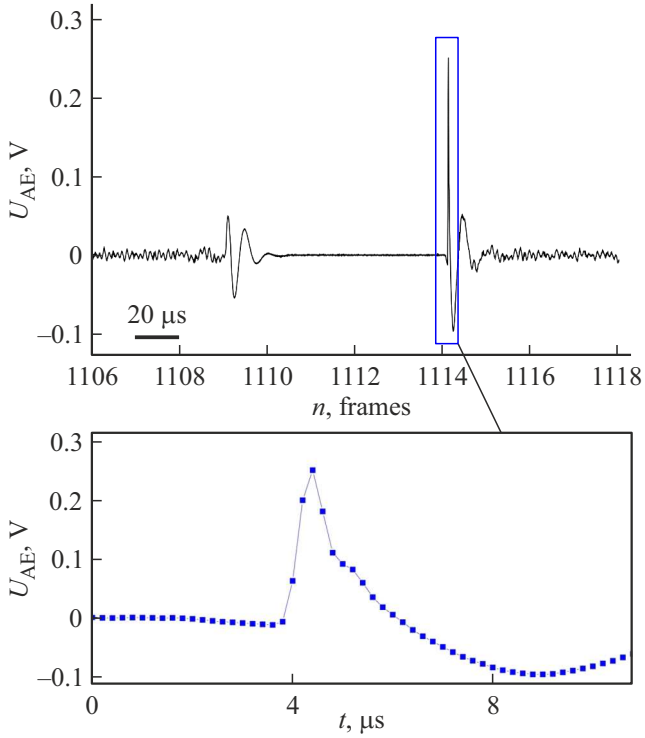

Figure 4. Waveform of acoustic signal $U_{AE}(t)$, corresponding to the accelerated stage of the primary band embryo growth under a stress of 310 MPa. In the caption: AE pulse with a build-up time of 0.6 μs, caused by band reaching the opposite lateral surface of the sample.

The AE signal related to the dynamics of the primary band at a stress of $\sigma_0 = 310$ MPa is composed of only two discrete AE signals with build-up time of not more than $\sim 1\,\mu$s (Fig. 4). The first of them coincides with a small jerk of the tip speed (frame 1109) with an amplitude of ~ 3 m/s and indicates the start of the final accelerated growth stage of the embryo deformation band, and the second signal coincides to a precision of not more than 20 μs with the moment of the band tip impact on the lateral surface of the sample (Fig. 5). The length of the build-up time of the second pulse is not greater than 0.6 μs, and its amplitude is almost 5 times greater than the first pulse. According to video recording data, the band tip reaches the lateral surface at a moment of time corresponding to frame 1115, which gives the maximum tip speed of 33 m/s. Based upon the acoustic signal, the second high-amplitude AE pulse, presumably related to the band tip impact on the lateral surface, is generated at a moment of time between frames 1114 and 1115. Taking into account this fact, the estimated maximum tip speed becomes twice higher, i.e., not less than up to 60 m/s.

It is worth noting, that in an interval of 220 μs between two microsecond pulses the level of acoustic noise is decreased by more than an order of magnitude (see Fig. 4). After the end of the second high-amplitude AE pulse the noise returns to its initial level. This „internal" absorption

of the intrinsic acoustic noise, or more specifically, the continuous component of the acoustic emission, may be related to the generation of a large number of movable dislocations at the stage of accelerated growth stage of the incomplete deformation band.

To study the mobility of dislocations in a band, it is important to know the dependence of dislocation speed in the band on the applied stress — the key dynamic characteristic of dislocations [30]. Fig. 6 shows the maximum embryo band tip speed $\upsilon_t^{\max}$ as a function of applied stress σ. If we assume the tip speed as a lower estimate of dislocation speed at the tip of incomplete band, then absolute values of $\upsilon_t^{\max}$ and linear behavior of its dependence on stress are indicative of viscous motion of dislocations of the head group.

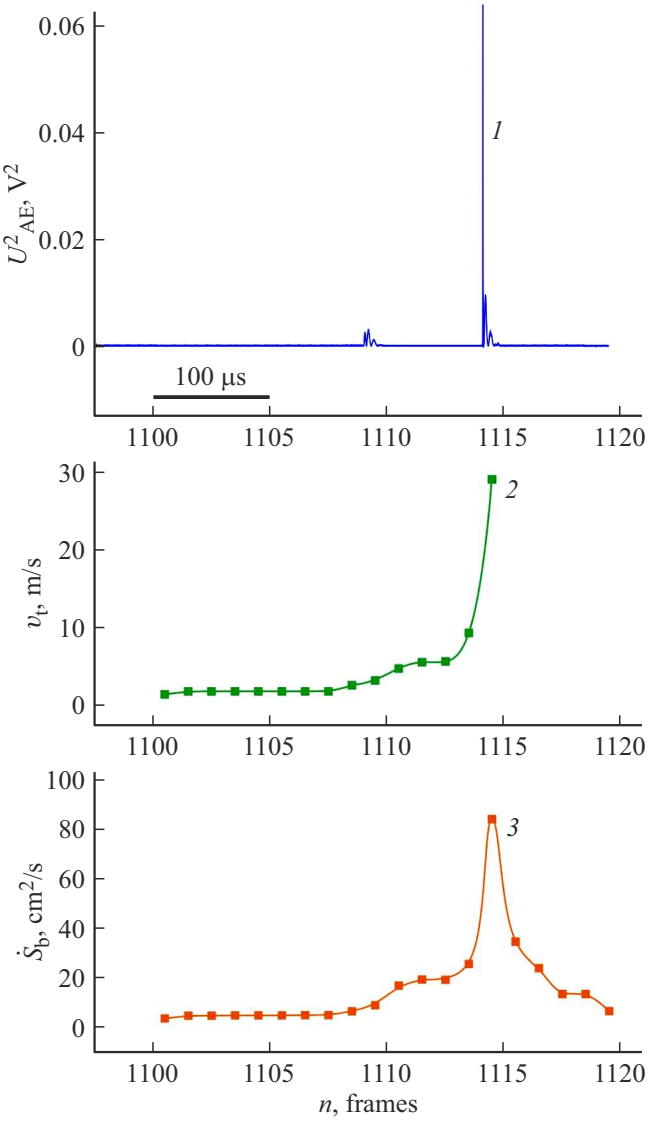

Figure 5. Correlation between the high-frequency acoustic signal in units of U^2_{AE} (curve *1*) and the tip speed υ_t (*2*) and the band area growth $\dot{S}_b(t)$ (*3*). Video recording rate is 50000 fps. Time interval between frames is 20 μs.

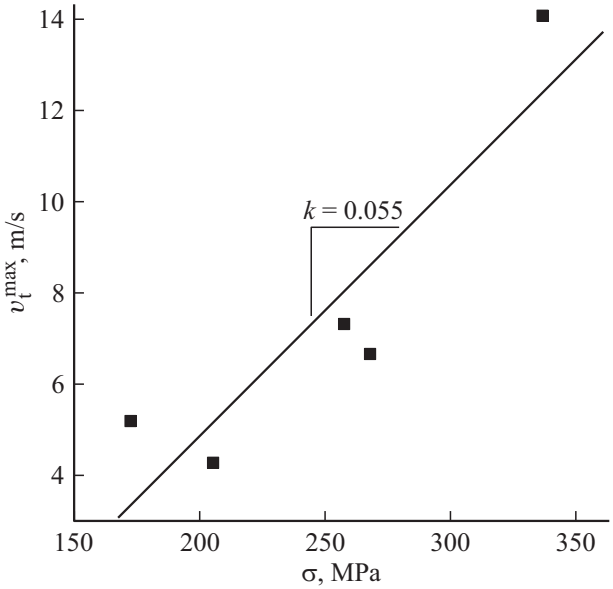

Figure 6. Maximum band tip speed as a function of applied stress $\upsilon_t^{\max}(\sigma)$. $k = 5.5 \cdot 10^{-2}$ m/MPa · s.

In the approximation of the viscous motion of dislocations

$$\upsilon_d = \frac{\sigma b_d}{B}, \tag{2}$$

where B — coefficient of dynamic dragging of dislocations, b_d — value of the Burgers vector for dislocation, υ_d — speed of dislocations [31]. Assuming $\upsilon_d \approx \upsilon_t$, we obtain an upper estimate of the coefficient of dynamic dragging of dislocations $B = b_d/k$, where $k = \Delta\upsilon_t^{\max}/\Delta\sigma = 5.5 \cdot 10^{-8}$ m/Pa · s — slope coefficient of the $\upsilon_t^{\max}(\sigma)$ dependence in Fig. 6. By substituting $b_d = 2.85 \cdot 10^{-10}$ m, we obtain $B \approx 5.4 \cdot 10^{-3}$ Pa · s, which is considerably greater than the value of B for individual dislocations in metals [30,31] and can qualitatively explain the strong absorption of the continuous component of the AE signal at the stage of accelerated growth of the embryo band. In the following section we shall present an estimate for the coefficient of dynamic dragging of dislocations within the model of non-linear growth of the embryo band.

3.3. Model of non-linear growth of PLC embryo band

Let us consider non-linear aspects of the dynamics of an individual deformation band in a thin plate expanded by a stress of $\sigma_0 = \text{const}$. We shall use the analogy with a crack, taking into account that in geometric and kinetic aspects the growth of the embryo band demonstrates a behavior similar to that of a growing crack: elliptic shape, presence of a stage of accelerated growth similar to the stage of supercritical growth of a crack [32]. As a result of the crack crossing through the sample bulk the stress relaxes by a value of expanding stress σ_0, and when the sample bulk is

crossed by an embryo band, the expanding stress relaxes by a stress serration of $\Delta\sigma$ on the deformation curve. We shall simulate the embryo band as an elliptic crack crossing the sample bulk, to which an expanding stress $\Delta\sigma$ is applied. Then the known formula for stress in the elliptic crack tip $\sigma_{\text{cr}} = \sigma_0(1 + 2a_{\text{cr}}/b_{\text{cr}})$ [33] (where a_{cr} and b_{cr} — semi-major and semi-minor axes of the crack) should be written for the embryo band as follows

$$\sigma_t = \Delta\sigma(1 + 2a/b), \tag{3}$$

where σ_t — stress in the embryo band tip, a and b — corresponding values for the embryo band, i.e,. a — band length, $2b$ — width at the band source on the lateral surface of the sample.

As it follows from the results of high-speed study of embryo band dynamics in AlMg6 alloy, the maximum tip speed is $\upsilon_t \approx 10-60$ m/s, i.e., it is in the range of a viscous motion of dislocation, while the speed of transversal growth is $\upsilon_s \approx 10-30$ cm/s, which is within the range of predominantly thermoactivated motion of dislocation when $\upsilon_s \propto \sigma_0^m$, where m is a constant value. Meanwhile, at the beginning stage of the band growth, dislocation speeds at the tip and even more on lateral boundaries of the band are not high yet ($\ll 1$ m/s), all dislocations of the band perform thermoactivated motion in the field of random obstacles — impurity atoms. Then $\upsilon_t/\upsilon_s \propto (\sigma_t/\Delta\sigma)^m \approx (2a/b)^m = \text{const}$, and the band moves with its elliptic shape remained. It is worth noting, that in the mode of the thermoactivated motion of dislocations the phenomenon of dynamic strain aging (DSA) is possible, i.e., dynamic interaction of dislocations with diffusing atoms of the impurity, which is usually used to explain the autolocalization of deformation in PLC bands [34].

When tip speed becomes higher than $\sim 1-10$ m/s, the dynamics of the embryo band is changed to the „mixed“ mode: dislocations in the band tip will move predominantly in a viscous manner, while dislocations on lateral boundaries will move in the thermoactivated mode. In the viscous mode dislocations perform over-barrier motion, which is not prone to DSA. As a result, dislocations in the band tip move considerably faster than those near the lateral boundary of the band. Since $\upsilon_s \ll \upsilon_t$, we shall assume for a first approximation that at this stage of growth the band width remains constant — $2b \approx \text{const}$, and dynamics of the band will be determined mainly by the tip speed. By combining equations (2) and (3), and taking into account that $\upsilon_d \approx \upsilon_t = \dot{a}$, $b = \text{const}$, $a \gg b$, we obtain

$$\frac{da}{dt} = C_1 a, \tag{4}$$

where $C_1 = 2\Delta b_d/Bb$. For time' dependencies of length and speed of the band we obtain, respectively,

$$a(t) = a_0 \exp(t/\tau), \tag{5}$$

$$\dot{a}(t) = \upsilon_t(t) = \upsilon_{t0} \exp(t/\tau), \tag{6}$$

where a_0 and $\upsilon_{t0} = a_0/\tau$ — length and speed of the band at the beginning of exponential growth of the band tip, and

$$\tau = C_1^{-1} = Bb/2\Delta\sigma b_d \tag{7}$$

— time constant of the exponential growth. By substituting in (7) typical values of experimental data: $\Delta\sigma = 10$ MPa, $b = 0.2$ mm, $\tau \approx 0.13$ ms, $b_d = 2.85 \cdot 10^{-10}$ m, we obtain an estimate of the dynamic dragging coefficient for the dislocations in the embryo band

$$B = 2\tau\Delta\sigma b_d/b \approx 3.7 \cdot 10^{-3}\ \text{Pa} \cdot \text{s}, \tag{8}$$

which is by 1.5–2 orders of magnitude greater than typical values of B for individual dislocations in aluminum as measured by various methods [31] and better than by an order of magnitude matching the estimate of B from the experimental dependence of the maximum band tip speed on the applied stress (see Fig. 6).

Note that in the interval of the accelerated embryo band growth in question, a strong absorption of the continuous AE component takes place. The abrupt increase in the coefficient of dynamic dragging of dislocations in the deformation band may be relayed to the intensive multiplication of dislocations and the thermal effect, which is well-known from thermal imaging of deformation band dynamics [35,36]. Thus, the model explains the exponential growth (see (1) and (6)) observed within the final third of the embryo band growth. This stage is preceded by an approximately linear growth of the band tip speed, that can be explained by assuming that the band grows with the tip radius unchanged $r_t = b^2/a = \text{const}$. Then $\Delta\sigma_t \approx 2\Delta\sigma\sqrt{a/r_t}$ and

$$\frac{da}{dt} = 2C_2\sqrt{a}, \tag{9}$$

where $C_2 = \Delta\sigma b_d/B\sqrt{r_t}$. Solution to (9) gives parabolic growth of the band length $a = C_2^2 t^2$ and, respectively, linear growth of the tip speed $\dot{a} = \upsilon_t(t) = 2C_2^2 t$.

Stages of embryo band reaching the surface. As the band tip approaches the opposite lateral surface, the „live cross-section“ of the sample decreases, which should result in an additional growth of stress at the band tip and its self-acceleration before reaching the sample surface. Since the „live“ cross-section tends toward zero in this case, singular behavior of the tip speed can be expected at the moment of the band reaching the outer surface.

Let us rewrite formula (3) taking into account the dependence of applied stress on the relative distance between the embryo band tip and the opposite surface $x = a/L_0$, where L_0 — width of the sample in the direction of the band growth $L_0 = a_{\max}$.

$$\sigma_t = \frac{\Delta\sigma(1 + 2a/b)}{1 - x}. \tag{10}$$

The equation for the band growth taking into account the condition of $a \gg b$ can be written as follows

$$\upsilon_t = \frac{C_1 L_0 x}{1 - x}. \tag{11}$$

The limit speed of dislocations according to [37] is $\upsilon_{d\max} \approx 0.5c_t$, where c_t — speed of transversal acoustic waves. Taking into account that $c_t = 3050$ m/s for aluminum [39], we obtain than dislocations in the band tip reach their maximum speed of $\upsilon_{d\max} \approx 1.5$ km/s at a distance of $L_0 - a_{\lim} = L_0/(1 + c_t/2C_1L_0) \approx 100\,\mu$m from the opposite edge, which they cover within $\Delta t \approx 80$ ns. Thus, the singularity of (11) is „eliminated" by the relativistic effect: band speed achieves its maximum at a distance of

$$a_{\lim} = \frac{L_0 c_t}{c_t + 2C_1 L_0} \approx 97.4\%L_0, \tag{12}$$

and the rest of the distance $\Delta a = L_0 - a_{\lim} \approx 2.6\%L_0$ is covered by the band tip at a limit speed of $\upsilon_{t\max} \approx 0.5c_t$ within approximately $0.1\,\mu$s before reaching the sample surface.

In addition to the relativistic effect, there are another factors affecting the speed of dislocations at the band tip, that are related to the competition between the image force attracting the dislocations to the surface and the repulsion force from the surface covered with a stronger layer of Al_2O_3 oxide (corundum) with a shear modulus almost by an order of magnitude greater than the shear modulus of aluminum ($G_{Al_2O_3} \gg G_{Al}$) [38]. The equilibrium between these forces is at a distance of about oxide film thickness $\delta \approx 10$ nm [37]. Thus, the presence of oxide impedes the dislocation outlet onto the surface. Although corundum has a higher shear modulus, its bending strength is low (about 220 MPa), therefore the oxide film is easily destroyed in the area of the stage related to the dislocations pule-up outlet. After the brittle oxide destruction, the dislocations are accelerated additionally by the image forces.

It is worth noting, that in case of „heterogeneous" band nucleation at the boundary of the preceding band, the source of the new band is located within the band boundary width, i.e., within the size of one or several grains [39]. In the process of evolution of an embryo band, its volume increases $V_b/V_g \approx 10^6$ times, where $V_b \approx L_b w_b \delta \approx 1\,\text{mm}^3$ is the band volume ($L_b = a(t_{\text{cr}}) \approx 4$ mm is finite length of the band, $w_b = 2b(t_{\text{cr}}) \approx 0.5$ mm is the width of the band, and $\delta = 0.5$ mm is the thickness of the sample), while $V_g \approx (\bar{d}) \approx 10^{-6}\,\text{mm}^3$ is an average grain volume, where $\bar{d} \approx 10\,\mu$m. Therefore avalanche-like multiplication of dislocations is a predominant (perhaps, not single) mechanism of the embryo band evolution. As a result of actuating of the Frank–Read (F–R) type dislocation source (typical for face-centered cubic (FCC) metals) in the „mother" grain near the sample surface, a flat pule-up of dislocations is generated, being locked by the grain boundary. To explain positive feedback, it is necessary to take into consideration the fact that at the phase of braking of the pule-up at the grain boundary an overstress pulse is generated and a local heating takes place that stimulates actuating of F–R sources in several adjacent grains, which may result in a „chain explosion" of a quantity of new dislocation pule-ups.

Comparison with AE signal. It is known that energy released in the course of AE event is approximately proportional to the volume of source [40], in this case to V_b. Hence, the energy of the acoustic signal

$$E = \frac{1}{R}\int_0^{t_0} U_{\text{AE}}^2(t)dt = \alpha V_b, \tag{13}$$

generated by an embryo band should be at least by 6 orders of magnitude greater than the AE energy from the F–R source in the mother grain (here R — electrical resistance of measuring circuit, t_0 — time of AE event, α — constant value). Therefore the moment of band nucleation can not be detected by the AE method: the expected signal is considerably lower than the level of acoustic noise in these conditions of deformation, which is the sum of the test machine noise and the continuous AE component of plastic deformable volume of the sample out of the growing embryo band. The major portion of the acoustic energy is released at the final stage of the embryo band growth, which is characterized by the maximum speed of the band volume growth $\dot{V}_b = \dot{S}_b\delta$.

By differentiating the acoustic signal energy (13) with respect to time, we get

$$U_{\text{AE}}^2 \propto \dot{V}_b = \dot{S}_b\delta = \pi \dot{a} b \delta \propto \upsilon_t, \tag{14}$$

i.e., the square amplitude of AE signal $A^2 = \left(U_{\text{AE}}^{\max}\right)^2$ is proportional to the speed of the band tip and according to (11) it tends to the maximum value (peak) in accordance with the following law

$$A^2(x) \propto \frac{x}{1-x} \tag{15}$$

with $x \to x_{\lim} = a_{\lim}/L_0$.

The source of peak AE signal is the final stage of the embryo band growth, i.e., the stage of reaching the opposite surface of the sample with a duration of $\Delta t \approx 2(L_0 - a_{\lim})c_t \approx 10^{-7}$ s, when dislocations in the band tip move at their limit speed of $\sim 0.5c_t$. The recorded peak of AE signal at the moment of the embryo band outlet onto the surface and its qualitative explanation with the scope of this model confirms (in addition to [41]) the mechanism of AE generation at the moment of dislocations outlet onto the surface of the crystal [42,43] as applicable to PLC deformation bands.

Thus, the proposed phenomenological model of the nonlinear growth of the embryo band explains qualitatively the main experimental results of high-speed studies *in situ* of dynamics of these bands using the example of aluminum-magnesium alloy: exponential growth of the band tip speed at the final stage before outlet onto the opposite lateral surface of flat sample, maximum amplitude of microsecond AE pulses at the moment of the band outlet onto the surface and acoustic noise absorption at this stage presumably related to the intensive multiplication of dislocations in the band.

4. Conclusion

Millisecond dynamics of the Portevin–Le Chatelier embryo bands was investigated experimentally by the method of high-speed video recording of the surface of a deformed sample of AlMg6 aluminum-magnesium alloy and synchronously by the AE method. Usually, the duration of the embryo band growth is not greater than a few milliseconds, therefore experimental study of this process requires methods with an action speed considerably higher than ~ 1 kHz. In this study we used high-speed video recording of the surface at a rate from 25000 to 50000 fps with a spatial resolution of up to $10\,\mu$m/px and AE measurement in a range of up to ~ 1 MHz.

The main results obtained in this work can be summarized as follows:

1. Embryo bands in flat samples are distinguished by their geometry and dynamics into 4 main types: primary bands growing transversally to the frontal surface in the direction of maximum tangential stresses; secondary bands growing along the boundary of the preceded band; secondary associated bands crossing preceded bands at an angle of about 60°, and arc-shaped bands growing in the area of blades. The first two types are characterized by the fastest dynamics, the last type is characterized by the slowest dynamics under the same level of applied stress. All types of embryo bands demonstrate non-linear dynamics with abrupt acceleration at the final stage of the growth.

2. Geometry and dynamics of the first two types are the same: more than half of the flat sample cross-section the embryo band tip grows at an almost linearly increasing speed of υ_t in the direction of maximum tangential stresses, then the stage of non-linear growth of the tip starts, that follows the exponential law of $\upsilon_t \propto \exp(t/\tau)$, where $\tau \approx 0.1-0.2$ ms is time constant of the accelerated growth. The band tip achieves its maximum speed at the moment of band outlet onto the opposite surface of the flat sample. The value of the maximum speed is frequently limited by the rate of video recording: $\sim 3-5$ m/s at a recording rate of 500 fps, $\sim 10-15$ m/s at 25000 fps, and $\sim 30-40$ m/s at 50000 fps.

3. It was found that the source of deformation band is located within one or several adjacent grains, and in the course of the embryo band growth its volume increases by more than six orders of magnitude, therefore the predominant mechanism of growth is the avalanche-like multiplication of dislocations. It is shown that dislocations in the embryo band tip at the stage of accelerated growth move in a quasi-viscous mode, and the transversal growth takes place due to the thermoactivated motion of dislocations.

4. Speed of the band tip achieves its maximum at the moment of outlet onto the opposite surface of the sample. At this moment the signal of acoustic emission achieves its peak value. Short series of microsecond AE pulses in the structure of the acoustic flash record the stage of the accelerated growth of embryo bands to a precision of $\sim 1\,\mu$s at high stresses, and the AE pulse with the maximum amplitude indicates the impact interaction of the embryo band with the sample surface. At the same time, the AE signal from band nucleation in the mother grain (grain cluster) is considerably lower than the level of continuous AE component related to the stochastic dynamics of dislocations pule-ups in grains of the plastic deformed sample. An abrupt absorption (by more than an order of magnitude) of acoustic noise was found at the stage of an accelerated growth of the embryo band, which may be related to the generation of a large quantity of movable dislocations.

5. A model of the embryo band non-linear growth is proposed that explains the experimentally observed exponential stage of the embryo band self-acceleration and forecasts the stage of band outlet onto the opposite surface, which is hard for experimental study, with a limit reativistic speed of the tip commensurable with the speed of shear waves in metal. An estimate of the coefficient of dislocation dynamic dragging at the band tip is made that is by $1.5-2$ orders of magnitude higher than the corresponding value for individual dislocations in aluminum, which presumably is related to the generation of a large number of new dislocations in the structure of the growing embryo band at the stage of its accelerated growth.

Funding

An analytical part of this study was partly supported by the Russian Science Foundation (project No. 22-22-00692), while experimental studies were performed using equipment of the Research Equipment Sharing Center of the G.R. Derzhavin Tambov State University with the support of the Ministry of Science and Higher Education of the Russian Federation within the project under agreement No. 075-15-2021-709 (unique project identifier RF-2296.61321X0037).

Conflict of interest

The authors declare that they have no conflict of interest.

References

[1] F. Savart. Ann. Chim. Phys. **65**, 337 (1837).
[2] E.N. da Costa Andrade. Proc. Royal Soc. A **84**, 1 (1910).
[3] A. Portevin, F. Le Chatelier, C.R. Acad. Sci. Paris **176**, 507 (1923).
[4] K. Chihab, Y. Estrin, L.P. Kubin, J. Vergnol. Scripta Met. **21**, 2, 203 (1987).
[5] A.A. Shibkov, A.E. Zolotov. Pis'ma v ZhETF **90**, *5*, 412 (2009) (in Russian).
[6] A.A. Shibkov, M.F. Gasanov, M.A. Zheltov, A.E. Zolotov, V.I. Ivolgin. Int. J. Plast. **86**, 37 (2016).
[7] A.J. Yilmaz. Sci. Technol. Adv. Mater. **12**, *6*, 063001 (2011).
[8] L.S. Derevyagina, V.E. Panin, A.I. Gordienko. Phiz. mezomekh. **10**, *4*, 59 (2007) (in Russian).
[9] A.A. Shibkov, A.E. Zolotov, M.A. Zheltov, A.V. Shuklinov, A.A. Denisov. FTT **53**, *10*, 1873 (2011) (in Russian).

[10] A.A. Shibkov, M.A. Zheltov, A.E. Zolotov, A.A. Denisov. FTT **53**, *10*, 1879 (2011) (in Russian).
[11] A. Chatterjee, A. Sarkar, P. Barat, P. Mukherjee, N. Gayathri. Mater. Sci. Eng. A **508**, *1*, 156 (2009).
[12] F.B. Klose, A. Ziegenbein, F. Hagemann, H. Neuhäuser, P. Hähner, M. Abbadi, A. Zeghloul. Mater. Sci. Eng. A **369**, *1–2*, 76 (2004).
[13] R. Shabadi, S. Kumar, H.J. Roven, E.S. Dwarakadasa. Mater. Sci. Eng. A **382**, *1–2*, 203 (2004).
[14] H. Louche, P. Vacher, R. Arrieux. Mater. Sci. Eng. A **404**, *1–2*, 188 (2005).
[15] H. Ait-Amokhtar, C. Fressengeas, S. Boudrahem. Mater. Sci. Eng. A **488**, *1–2*, 540 (2008).
[16] A.A. Shibkov, A.E. Zolotov, M.A. Zheltov, A.A. Denisov, M.F. Gasanov. ZhTF **84**, *4*, 40 (2014) (in Russian).
[17] W. Tong, H. Tao, N. Zhang, L.G. Hector Jr. Scripta Mater. **53**, 87 (2005).
[18] G.F. Xiang, Q.C. Zhang, H.W. Liu, X.P. Wu, X.Y. Ju. Scripta Mater. **56**, 721 (2007).
[19] M.M. Krishtal, A.K. Khrustalev, A.V. Volkov, S.A. Borodin. Dokl. Phys. **54**, *5*, 225 (2009).
[20] A.A. Shibkov, M.A. Zheltov, M.F. Gasanov, A.E. Zolotov. FTT **59**, *12*, 2363 (2017) (in Russian).
[21] A.A. Shibkov, M.A. Zheltov, M.F. Gasanov, A.E. Zolotov, A.A. Denisov, M.A. Lebyodkin. Mater. Sci. Eng. A **772**, 138777 (2020).
[22] A.A. Shibkov, A.E. Zolotov. Kristallografiya **56**, *1*, 147 (2011) (in Russian).
[23] A.H. Cottrell. Trans. Met. Soc. AIME **38**, *2*, 192 (1958).
[24] J. Zdunek, T. Brynk, J. Mizera, Z. Pakiela, K.J. Kurzydlowski. Mater. Charact. **59**, 1429 (2008).
[25] M.A. Lebyodkin, D.A. Zhemchuzhnikova, T.A. Lebedkina, E.C. Aifantis. Res.Phys. **12**, 867 (2019).
[26] V.V. Gorbatenko, V.I. Danilov, L.B. Zuev. Technical Phys. **62**, *3*, 395 (2017).
[27] D. Yuzbekova, A. Mogucheva, Y. Borisova, R. Kaibyshev. J. Alloys. Compounds **868**, 159135 (2021).
[28] R. Hill. Matematicheskaya teoriya plastichnosti. Gostechizdat, M. (1956). 408 s. (in Russian).
[29] H.M. Zbib, E.C. Aifantis. Scripta Met. **22**, *8*, 1331 (1988).
[30] V.I. Nikitenko. In: Nesovershenstva kristallicheskogo stroeniya I martensitnye prevrashcheniya. Nauka, M. (1972). S. 136 (in Russian).
[31] V.I. Al'shits, V.L. Indenbom. UFN **115**, *1*, 3 (1975) (in Russian).
[32] V.M. Pestrikov, E.M. Morozov. Mekhanika razrusheniya rvyordykh tel. Professiya,SPb (2002). 320 s. (in Russian).
[33] V.Z. Parton, E.M. Morozov. Mekhanika uprugoplasticheskogo razrusheniya: Osnovy mekhaniki razrusheniya. LKI, M. (2008). 352 s. (in Russian).
[34] L.P. Kubin, C. Fressengeas, G. Ananthakrishna. Dislocat. Solids **11**, 101 (2002).
[35] H. Ait-Amokhtar, C. Fressengeas. Acta Materialia **58**, *4*, 1342 (2010).
[36] R. Nogueira de Codes, O.S. Hopperstad, O. Engler, O.-G. Lademo, J.D. Embury, A. Benallal. Metall. Mater. Trans. A **42**, *11*, 3358 (2011).
[37] Zh. Fridel'. Dislokatsii. Mir, M. (1976). 660 s. (in Russian).
[38] Tablitsy fizicheskikh velichin. Handbook / Eds. I.K. Kikoina. Atomizdat, M. (1976). 1008 s. (in Russian).
[39] A.A. Shibkov, A.E. Zolotov, M.A. Zheltov. FTT **52**, *11*, 2223 (2010) (in Russian).
[40] A.G. Beattie. Acoustic emission non-destructive testing of structures using source location techniques. Sandia National Laboratories, Albuquerque, NM (2013).
[41] V.S. Boyko, V.F. Kivshik, L.F. Krivenko. ZhETF **82**, *2*, 504 (1982) (in Russian).
[42] V.D. Natsik. Pis'ma v ZhETF **8**, *3*, 198 (1968) (in Russian).
[43] V.D. Natsik, K.A. Chishko. Akust. zhurn. **28**, *3*, 381 (1982) (in Russian).